# Coherent beam-beam interaction with four colliding beams

B. Podobedov and R. H. Siemann
*Stanford Linear Accelerator Center, Stanford University, Stanford, California 94309*
(Received 4 November 1994; revised manuscript received 12 April 1995)

The coherent beam-beam interaction in the absence of Landau damping is studied with a computer simulation of four space-charge-compensated colliding beams. Results are presented for the modes, phase space structures, widths, and growth rates of coherent beam-beam resonances. These results are compared with solutions of the Vlasov equation, and with measurements made at the Dispositif de Collisions dans l'Igloo (DCI) storage ring in Orsay, France, which operated with space-charge-compensated colliding beams.

PACS number(s): 29.27.Bd, 29.20.Dh

## INTRODUCTION

The luminosity of storage ring colliders is limited by the effects of the electromagnetic fields of one beam on the particles of the other beam. This beam-beam interaction is parametrized by the beam-beam strength parameter,

$$\xi=\frac{r_e}{2\pi}\frac{N\beta_y^*}{\gamma\sigma_y(\sigma_x+\sigma_y)}\ , \tag{1}$$

where $r_e$ is the classical electron radius, $N$ is the number of particles in the beam, $\beta_y^*$ is the vertical amplitude function at the interaction point, $\gamma$ is the beam energy in units of rest energy, and $\sigma_x$ and $\sigma_y$ are the rms horizontal and vertical beam sizes at the interaction point. The beam-beam interaction is not linear in displacement, and, in the usual case of two colliding beams, those nonlinearities introduce single particle nonlinear resonances and a spread in transverse oscillation tunes. The vertical tune spread is equal to $\xi$, which is sometimes denoted as $\xi_y$. The beam-beam luminosity limit could be due to the nonlinear resonances and the tune spread, which are single particle, incoherent effects, or it could be due to coherent instabilities [1].

Coherent beam-beam instabilities are expected based on solutions of the Vlasov equation [2–5]. They are characterized by rapid, turn-by-turn, correlated variations of the beam distributions. They have been seen in a two-beam simulation that used particle-in-cell techniques to calculate electromagnetic fields [6]. In this simulation there was qualitative agreement with Vlasov equation solutions for sixth and eight order resonances, but higher order resonances were not seen, presumably because of Landau damping from the beam-beam tune spread. The instabilities that were observed occurred for $\xi \geq 0.05$ and could be avoided by the appropriate choice of operating point. This led to the conclusion that the coherent beam-beam effect was not likely to be important in operating or planned colliders. In contrast, turn-by-turn variations of beam sizes have been observed at LEP using a detector capable of imaging the beam on successive turns [7]. More data are needed before drawing any conclusion about the relation between these variations and the beam-beam limit.

Incoherent beam-beam effects can be eliminated by colliding four beams in the field compensating configuration shown in Fig. 1. Without incoherent effects there is a possibility of substantially improved performance. However, there is no Landau damping from the beam-beam tune spread, and coherent instabilities could be much more important. The DCI (Dispositif de Collisions dans l'Igloo) storage ring at the Laboratoire de l'Accélérateur Linéaire (Orsay, France) had four colliding, space-charge-compensated beams, and the beam-beam limit was not significantly different than with two beams [8]. This is a strong indication of the importance of coherent beam-beam effects in this configuration, and the DCI performance limit was attributed to them.

This paper reports the results of a computer simulation of four colliding beams. Coherent beam-beam resonances are observed, and their mode structures, phase space structures, widths, and growth rates are measured and compared with solutions of the Vlasov equation to study the underlying physics of the coherent beam-beam interaction. Other results are compared with DCI measurements to understand the performance there.

## SIMULATION

The simulation is a modification of that of Krishnagopal and Siemann [6]. Test particles were followed in transverse, four-dimensional phase space for a large number of turns, with each turn consisting of transport between the interaction points and beam-beam collisions.

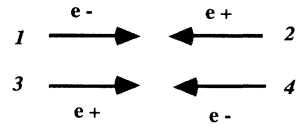


FIG. 1. Four colliding beams in the field compensation configuration used in DCI. The four beams are collinear and arrive at the interaction point at the same time.

 

The initial phase space coordinates were chosen from Gaussian distributions with the nominal sizes.

Different transport models were used based on the issue under study. For resonance studies and for comparisons with the Vlasov theory (i) the horizontal and vertical dimensions were independent, (ii) centroid feedback set the mean coordinates to zero before the beam-beam interaction, and (iii) there was no radiation damping or quantum excitation. The DCI simulations were intended for comparison with experiments, and the transport had coupling between horizontal and vertical motions, radiation damping, quantum excitation, and no centroid feedback. In addition, either one or two interaction regions was possible, and the two-interaction region model had phase advance errors between the interaction regions. These errors were consistent with estimates based on the DCI magnetic lattice with quadrupole gradient errors [9].

The electromagnetic fields at the collision point were calculated by Lorentz transforming to the rest frame of a pair of beams and solving for the electrostatic fields there. First, a circular mesh was constructed for each pair of beams. The meshes had 16 azimuthal bins and 100 radial bins each with a size $\Delta r=(\sigma_{x0}+\sigma_{y0})/20$ where $\sigma_{x0}$ and $\sigma_{y0}$ are the nominal horizontal and vertical rms beam sizes. Each mesh was centered; for example, the origin of the mesh for beams 1 and 3 was centered at $\bar{x}=(\bar{x}_1+\bar{x}_3)/2$ and $\bar{y}=(\bar{y}_1+\bar{y}_3)/2$, where $\bar{x}_1$ is the horizontal centroid of beam 1, etc.

Particles were placed on this mesh by apportioning them to adjacent mesh sites with area weighting fractions [10] and taking their charge into account. The resultant array was Fourier analyzed in azimuth, and the real and imaginary parts of the Fourier coefficients were smoothed to reduce the effects of statistical fluctuations in the number of test particles at individual mesh sites. The smoothing was performed with the IMSL routine CSSCV [11], which is based on a smoothing spline to approximate noisy data with the smoothing parameter found by cross validation [12]. The smoothed charge distributions together with the Green's function for Poisson's equation in polar coordinates gave the electrostatic fields.

## VLASOV THEORY FOR COHERENT INSTABILITIES OF FOUR COLLIDING BEAMS

### Introduction

There are several Vlasov equation solutions for the coherent beam-beam interaction. The initial work was by Derbenev and was devoted to four beams with transverse motion in two spatial dimensions [2]. Dikansky and Pestrikov considered two beams, two transverse spatial dimensions, and synchrotron motion [3]. Chao and Ruth studied two beams, only one transverse dimension, and no synchrotron motion [4]. Zenkevich and Yokoya calculated the growth rates for two beams and one-dimensional oscillations including Landau damping [5]. They found that the growth rates of low order resonances were diminished significantly by Landau damping.

There are qualitative disagreements between Chao and Ruth and Dikansky and Pestrikov when that calculation is restricted to one dimension. These disagreements arise from (i) different treatments of the focusing of the equilibrium distribution when making action-angle transformations (Chao and Ruth account for it while Dikansky and Pestrikov do not), and (ii) an implicit assumption by Dikansky and Pestrikov that perturbations cannot be defocusing. These disagreements do not affect the four-beam calculation.

### Vlasov equation solution of Derbenev (Ref. 2)

This section is a summary of the Derbenev paper. Some of the numerical coefficients in equations are different, and Derbenev numbers the beams differently than we do in Fig. 1. This leads to some sign differences in the equations. Neglecting radiation damping and synchrotron oscillations, the linearized Vlasov equations may be written in the form

$$\frac{\partial f_q}{\partial t}+\frac{2\pi}{T}Q_\alpha\frac{\partial f_q}{\partial\varphi_\alpha}=-\frac{\partial\tilde{L}_q}{\partial\varphi_\alpha}\frac{\partial F}{\partial I_\alpha}\ , \tag{2}$$

where $\{\varphi_\alpha,I_\alpha\}$ are action-angle variables, $T$ and $Q_\alpha$ are the revolution period and betatron tune, respectively, and there is a summation over index $\alpha$. All four beams are assumed to have the same equilibrium distribution $F$, and $f_q$ is the perturbation of the density distribution of beam $q$. The Lagrangian for interaction of a particle with fields excited by collective oscillations of other beams is $\tilde{L}_q$. For example, the Lagrangian of interaction of particle in beam 1 with the fields of beams 2 and 4 can be represented in the form

$$\tilde{L}_1(\mathbf{r}_\perp,t)=-4e^2\delta_T\int d\Gamma'_\perp[f_2(\mathbf{p}'_\perp,\mathbf{r}'_\perp,t)-f_4(\mathbf{p}'_\perp,\mathbf{r}'_\perp,t)]\ln(|\mathbf{r}_\perp-\mathbf{r}'_\perp|)\ , \tag{3}$$

where $\delta_T$ is a periodic delta function with period equal to the revolution period, $\mathbf{p}'_\perp$ and $\mathbf{r}'_\perp$ are transverse deviations from the equilibrium orbit, and $d\Gamma'_\perp$ is a phase space volume element.

The four-beam system can have four modes,

$$f^{\pm}_{+}=[f_1+f_3]\pm[f_2+f_4]$$

and (4)

$$f^{\pm}_{-}=[f_1-f_3]\pm[f_2-f_4]\ .$$

Instability develops from differences in the densities of the two beams moving in the same direction, so only two of these modes, the $f_-$ modes, can be unstable. The $-$ subscript is dropped in the equations that follow. The equations for the individual beams can be added and subtracted, leading to a set of uncoupled equations for $f^+$ and $f^-$. Stationary solutions of the form

$$f^{\pm}(\mathbf{I},\varphi,t+T)=\lambda f^{\pm}(\mathbf{I},\varphi,t) \tag{5}$$

are sought. They are unstable if $|\lambda|>1$. The phase space distribution is Fourier transformed in angle,

$$f(\mathbf{I},\varphi)=\sum_{\mathbf{m}}f_{\mathbf{m}}(\mathbf{I})\exp\{i\mathbf{m}\cdot\varphi\}\ . \tag{6}$$

TABLE I. Parameters for comparisons with Vlasov equation.

| Betatron tune, $Q=Q_x=Q_y$ | $\sim 0.8$ |
|---|---|
| Coupling | Independent horizontal and vertical motions |
| Radiation | No radiation damping or fluctuations |
| Feedback | Centroid Feedback, $\bar{x}_1=\bar{y}_1=\cdots=0$, before collisions |
| Number of test particles/beam, $N_{TP}$ | 50 000 |

The charge density is Fourier transformed,

$$\sigma(\mathbf{k})=\int dx \int dy\, e^{i\mathbf{k}\cdot\mathbf{r}}\left[\int dp_x \int dp_y f(\mathbf{I},\varphi)\right], \quad (7)$$

and the equilibrium distribution is assumed to be a Gaussian. The result is an integral equation for $f(\mathbf{k})=\sigma(\mathbf{k})/k$,

$$f^{\pm}(\mathbf{k})=\mp 4i\sum_{\mathbf{m}}\frac{\mathbf{m}\cdot\xi}{1-\lambda\exp(2\pi i\mathbf{m}\cdot\mathbf{Q})}\times\int g_{\mathbf{m}}(\mathbf{k},\mathbf{k}')f^{\pm}(\mathbf{k}')d^2\mathbf{k}', \quad (8)$$

that leads to resonances when $\mathbf{m}\cdot\mathbf{Q}$ is close to an integer. The kernel in this equation is

$$g_{\mathbf{m}}(\mathbf{k},\mathbf{k}')=\frac{4}{kk'}I_{m_x}(k_xk_x')I_{m_y}(k_yk_y')\exp\left[-\frac{k^2+k'^2}{2}\right]. \quad (9)$$

### Round beams

Our simulations have been done for the case of nominally round beams, beams with equal sizes initially ($\sigma_{x0}=\sigma_{y0}\equiv\sigma_0$), equal beam-beam strength parameters ($\xi_x=\xi_y=\xi$), and equal betatron tunes ($Q_x=Q_y\equiv Q$). This case can be analyzed by replacing the sums over $m_x$ and $m_y$ in Eq. (8) by sums over $m_x+m_y$ and $m_x-m_y$. The term in front of the integral in Eq. (8) depends only on $m_x+m_y$, and Eq. (9) can be summed over $m_x-m_y$ to give

$$f^{\pm}(\mathbf{k})=\mp 4i\sum_{m_x+m_y}\frac{(m_x+m_y)\xi}{1-\lambda\exp[2\pi i(m_x+m_y)Q]}\times\int g_{m_x+m_y}(\mathbf{k},\mathbf{k}')f^{\pm}(\mathbf{k}')d^2k', \quad (10)$$

with

$$g_{m_x+m_y}(\mathbf{k},\mathbf{k}')=\frac{4}{kk'}I_{m_x+m_y}(\mathbf{k}\cdot\mathbf{k}')\exp\left[-\frac{k^2+k'^2}{2}\right]. \quad (11)$$

There is nothing to distinguish the two transverse dimensions, and therefore the angularly symmetric harmonic $f_0$ in the Fourier expansion,

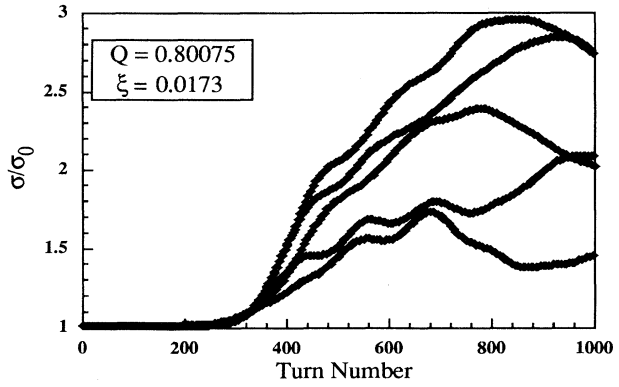


FIG. 2. The rms horizontal size of beam 1 normalized to the nominal size.

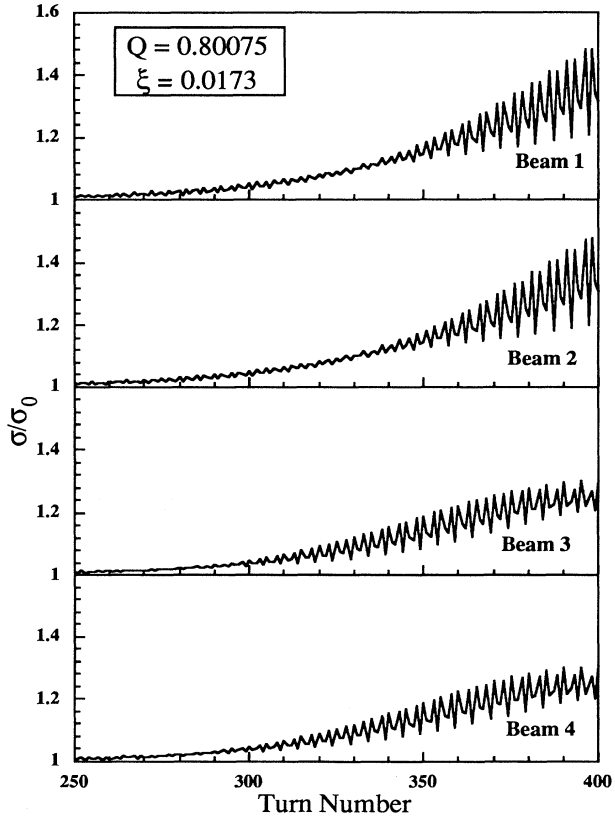


FIG. 3. Horizontal beam sizes for turns 250–400 where the instability appears.

$$f(\mathbf{k})=\sum_q f_q(k)e^{iq\theta}\ , \tag{12}$$

is expected to dominate for round beams. The integral in Eq. (10) equals zero for this harmonic when $m_x+m_y$ is odd, and only even order resonances with resonance condition

$$(m_x+m_y)Q=2mQ=n \tag{13}$$

are allowed. Equations (10) and (11) become

$$f_0^{\pm}(k)=\mp 16\pi i\xi\sum_m \frac{m}{1-\lambda\exp(4\pi imQ)} \times\int g_m^0(k,k')f_0^{\pm}(k')k'dk' \tag{14}$$

and

$$g_m^0(k,k')=\frac{4}{kk'}I_m^2\left[\frac{kk'}{2}\right]\exp\left[-\frac{k^2+k'^2}{2}\right]. \tag{15}$$

Equation (14) can be solved for $Q=n/2m+\Delta Q$ when $\Delta Q\ll 1$ by keeping only the $+m$ and $-m$ terms in the sum. Looking for eigenvalues of the form

$$\lambda=\exp[4\pi i(-mQ+\delta)] \tag{16}$$

gives

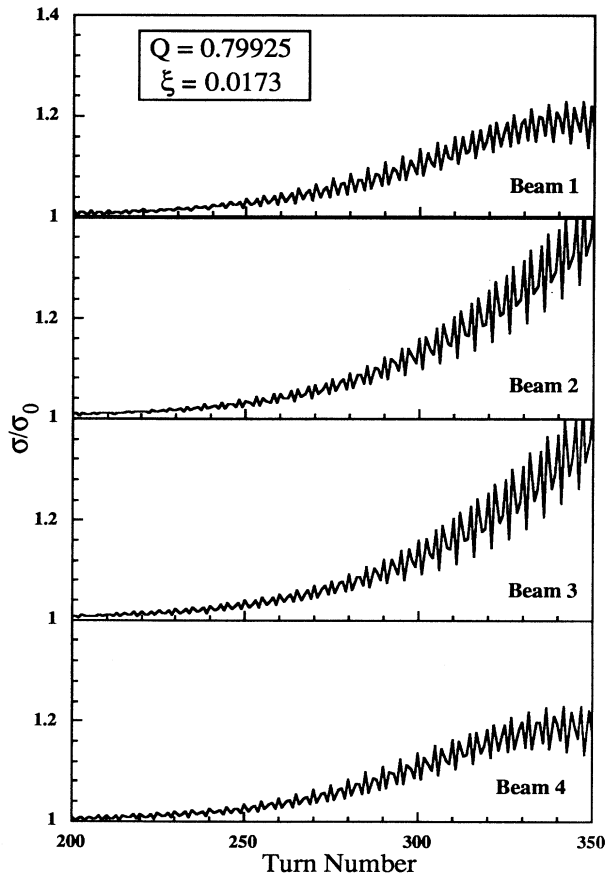


FIG. 4. Horizontal beams sizes on the other side of the $Q=\frac{8}{10}$ resonance.

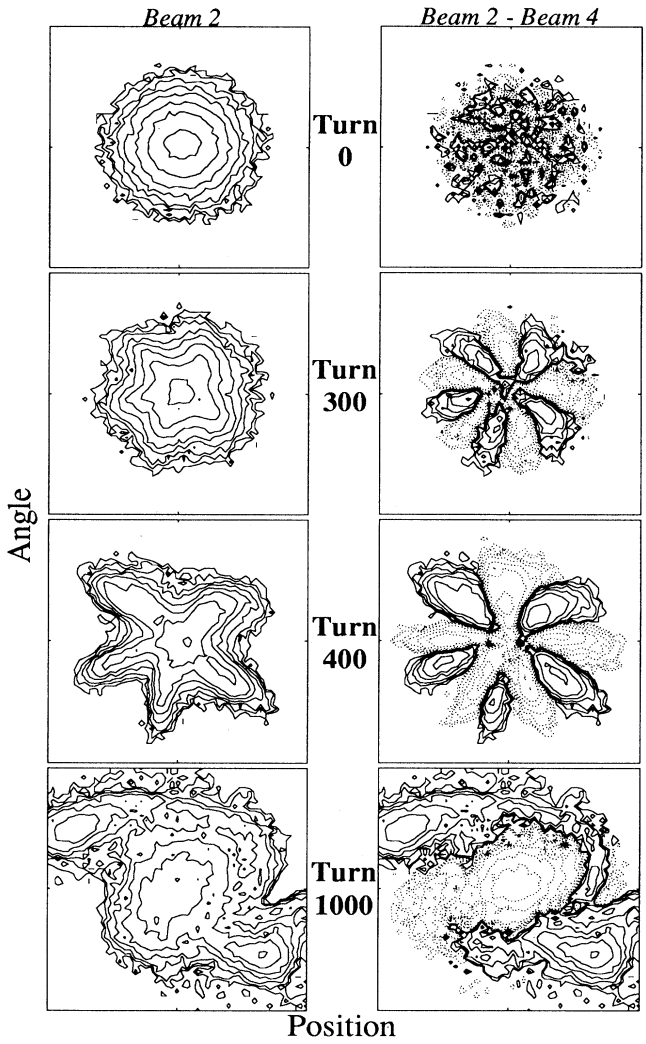


FIG. 5. Horizontal phase space plots for $Q=0.800\,75$ and $\xi=0.0173$ for beam 2 ($f_2$) on the left and for ($f_2-f_4$), the difference between beams 2 and 4, on the right. The plots cover $\pm 5$ times the nominal rms sizes, and the dashed lines are contours of negative value.

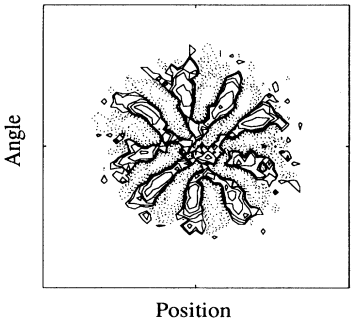


FIG. 6. Horizontal phase space contours of ($f_2-f_4$) for $Q=0.777\,853$ and $\xi=0.0173$, a point within the $Q=\frac{14}{18}$ resonance. The plots cover $\pm 5$ times the nominal rms sizes, and the dashed lines are contours of negative value.

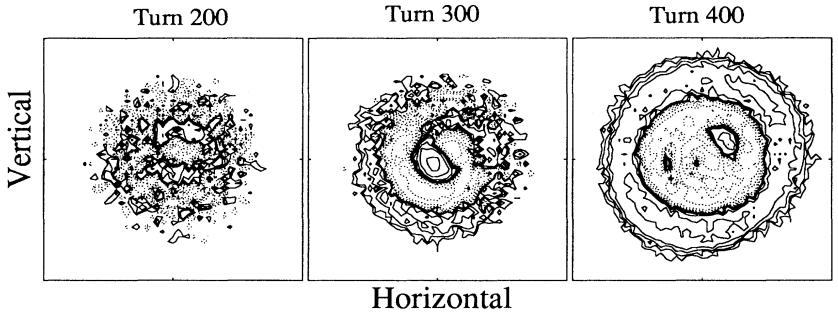


FIG. 7. Contour plots in physical space for $f_2-f_4$. The figures cover $\pm 5\sigma_0$, and the conditions are those of Fig. 4: $Q=0.79925$ and $\xi=0.0173$.

$$\delta = m\{\Delta Q \pm \sqrt{(\Delta Q)^2 \mp 8\xi C_m \Delta Q}\} . \quad (17)$$

The minus sign inside the square root holds for $f^+$, the plus sign holds for $f^-$, and $C_m$ is the eigenvalue of

$$C_m f_0(k) = \int g_m^0(k,k') f_0(k') k' dk' . \quad (18)$$

Equation (17) contains an essential result. The $f^+$ mode is unstable for tunes above the resonance, $0 \le \Delta Q \le 8\xi C_m$, and the growth rate is

$$\tau^{-1} = 4\pi m \sqrt{8\xi C_m |\Delta Q| - (\Delta Q)^2} . \quad (19)$$

The $f^-$ mode is unstable for tunes below the resonance, $-8\xi C_m \le \Delta Q \le 0$, with the growth rate given by Eq. (19).

Solving the eigenvalue equation numerically for different values of $m$ gives the parametrization

$$C_m = \frac{0.322}{m^{2.9}} \quad (20)$$

for the largest eigenvalue. We compare simulation results with the expressions for widths and growth rates using Eq. (20), although there are reservations in doing so: (i) Equation (20) is for the largest eigenvalue and other eigenvalues are comparable with roughly ten being able to make contributions to the width and growth rate, and (ii) we measure the growth rate of $\sigma^2-\sigma_0^2$, which is beyond the scope of the linearized Vlasov equation. In making these comparisons we are primarily interested in orders of magnitude and the dependence on resonance order.

## COMPARISONS WITH SIMULATIONS

An extensive study of the tenth order resonance $Q=\frac{8}{10}$ was performed using the parameters given in Table I. The nature of the coherent instability is illustrated in Figs. 2 and 3. The beam sizes are stable and equal to the nominal sizes for roughly the first 200 turns. They increase rapidly after that, eventually reaching a condition that repeats every fifth turn. The horizontal size of beam 1 is plotted in Fig. 2. Vertical sizes behave the same when the tunes are equal. As shown in Fig. 3, beams 1 and 2 behave identically as do beams 3 and 4. This is as expected since the tune is above the resonance value of $\frac{8}{10}$, and therefore the $f^+$ mode should be unstable. Figure 4 shows the sizes on the other side of $Q=\frac{8}{10}$, where the $f^-$ mode should be unstable. As expected in this figure beams 1 and 4 have the same behavior as do beams 2 and 3.

This resonance corresponds to $m=5$, and there should be fivefold structure in the horizontal and vertical phase

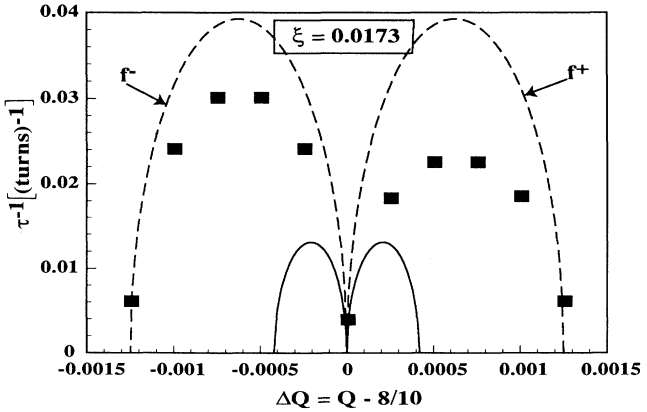


FIG. 8. The growth rate of $\sigma^2-\sigma_0^2$ from the simulation compared with Eq. (19) using the eigenvalue from Eq. (20) (solid line) and using three times that eigenvalue (dashed line).

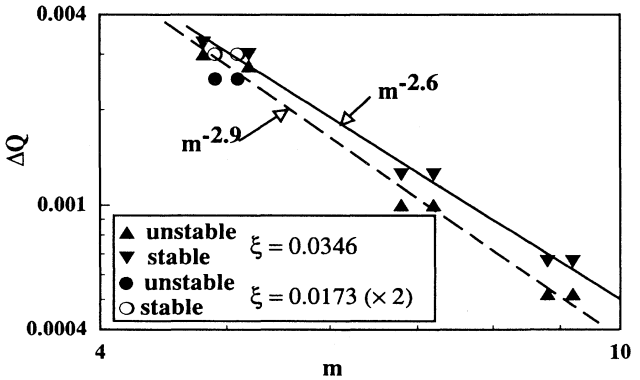


FIG. 9. Resonance widths for different resonance orders. The first stable and last unstable points on each side of the resonance are indicated. The resonances are $\frac{8}{10}$ ($m=5$), $\frac{11}{14}$ ($m=7$), and $\frac{14}{18}$ ($m=9$). The resonance width for $m=5$, $\xi=0.0173$ was doubled for inclusion in the figure.

TABLE II. Parameters of DCI models.

| Parameter | ONE | TWO |
|---|---|---|
| Interaction regions | 1 | 2 |
| $Q$ | ~0.88 | ~1.76 |
| $\beta^*$ (m) Horizontal | 2.18 | 2.18 |
| Vertical | 2.18 | 2.18 |
| $\varepsilon$ ($\mu$m) Horizontal | 0.282 | 0.282 |
| Vertical | 0.015 | 0.015 |
| Coupling resonance width [13] | 0.001 | 0.002 |
| Arc errors {horizontal, vertical} | | {0.0005, −0.002}, |
| Energy ($\gamma$) | $1.57\times10^3$ | $1.57\times10^3$ |
| Fractional energy loss per turn | $7.1\times10^{-6}$ | $14.2\times10^{-6}$ |
| Feedback | No feedback | No feedback |
| Nominal beam sizes ($\mu$m) | 569 (fully coupled) | 569 (fully coupled) |
| Number of test particles/beam, $N_{TP}$ | 10 000 | 10 000 |
| Turns of tracking | 20 000 | 10 000 |

spaces as the instability develops. This is seen clearly and is illustrated in Fig. 5 for $Q=0.800\,75$. The difference $f_2-f_4$ starts out essentially uniform. Fivefold structure has developed by turn 300. It persists during the rapid growth of beam size, but phase space has become badly distorted by the time the beam has reached its limiting behavior. The vertical phase space also has fivefold structure during the growth of the instability, and it evolves in a similar manner through turn 1000. Other resonances have phase space structure determined by the resonance order. Figure 6 is an example for the 18th order resonance $Q=\frac{14}{18}$.

The beams are nominally round, but there are no restrictions forcing them to stay round. However, they do remain round to a substantial degree, although some variation with the azimuthal angle in physical space does occur. This is illustrated in Fig. 7.

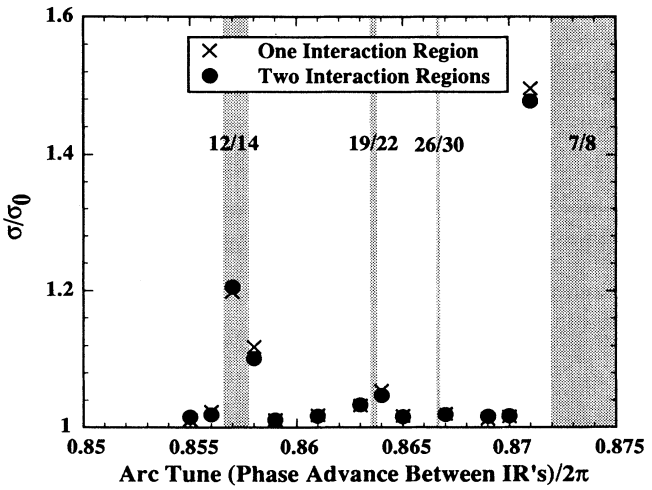


FIG. 10. rms beam size in DCI normalized to the nominal size for region I: $Q\sim0.865$, $\xi=0.0218$. Even order resonances up to 30th order are plotted with widths calculated using the $m$ dependence in Eq. (20) and a coefficient three times larger.

The instability growth rate was estimated by fitting the square of the beam size, corrected for the equilibrium size, $\sigma^2-\sigma_0^2$, with an exponential during the initial rise of the instability. This quantity was chosen for fitting since it is proportional to the emittance increase due to the instability. Figure 8 shows the results. The width is about three times that expected using the eigenvalue in Eq. (20). When three times that eigenvalue is used, the width agrees and the growth rate is about half that of Eq. (19). This is reasonable agreement given that comparable eigenvalues were neglected and that the connection between the growth rate given by Eq. (19) and the growth rate of $\sigma^2-\sigma_0^2$ is tenuous.

Note that the growth at $Q=\frac{8}{10}$ is not exactly zero, as would be expected. We found that the growth rates at the centers of resonances depend on the number of test particles and tend to zero as $N_{TP}^{1/2}$, where $N_{TP}$ is the number of test particles. The growth rate at $\Delta Q=-0.0005$, a point of maximum growth in Fig. 8, changed by less than 25% when the number of test particles was varied from 25 000 to 150 000.

Two other aspects of the Vlasov equation solution were studied. Odd order resonances were searched for and none were found, and resonance widths were measured by tracking for different values of $Q$ and $\xi$. The resultant dependence on resonance order is given in Fig. 9. The widths are linear in $\xi$, and they depend on $m$ as $m^{-2.6}$ to $m^{-2.9}$. This is in good agreement with the dependence expected from Eq. (20).

## DCI PERFORMANCE

Four DCI operating points documented by LeDuff *et al.* [8] were chosen for comparison between measurements and simulations. Two models of DCI, ONE and TWO, named after the number of interaction regions, were used. Reference [9] has details of these models. Parameters are given in Table II.

Figure 10 shows the results for one point, $Q=0.865$ and $\xi=0.022$. There are strong, low order resonances, $Q=\frac{12}{14}$ and $Q=\frac{7}{8}$, on the two sides of this operating

TABLE III. Comparison of measured and simulated widths of stable operating regions. Measured widths are from LeDuff *et al.* [8]. The entries are the stable operating regions from Fig. 3 of that reference divided by 2 for comparison with simulations of ONE.

| Region | I | II | III | IV |
|---|---|---|---|---|
| $Q$, $\xi$ | 0.865, 0.022 | 0.884, 0.018 | 0.894, 0.014 | 0.907, 0.011 |
| Measured width | 0.0020 | 0.0027 | 0.0027 | 0.0034 |
| Simulated width | 0.011 | 0.009 | 0.009 | 0.013 |
| Bounding resonances | $\frac{12}{14}$, $\frac{7}{8}$ | $\frac{7}{8}$, $\frac{16}{18}$ | $\frac{16}{18}$, $\frac{9}{10}$ | $\frac{9}{10}$, $\frac{11}{12}$ |
| Overlapped resonances (up to 30th order) | $\frac{19}{22}$, $\frac{26}{30}$ | $\frac{23}{26}$ | $\frac{25}{28}$ | $\frac{20}{22}$ |

point, leading to a region of width $\Delta Q \approx 0.011$, where the beam size has increased by less than 10% after tracking for 20 000 turns. This is to be compared with a measured stable operating region of $\Delta Q \approx 0.0020$, which was extracted from Fig. 3 of Ref. [8] and reduced by a factor of 2 for comparison with the one interaction region model. The measured widths for stable operation at the four operating points are compared with the widths from simulation in Table III. The simulation predicts stable regions 3–5 times wider than those measured.

The measurements themselves could be in error due to effects such as quadrupole power supply regulation, narrowing the observed stable operating point, but this cannot be tested and must remain speculation at best. Synchrobetatron resonances could play a role, but the DCI bunch length was short compared to $\beta^*$, and the dispersion at the interaction region was small [14]. There are indications that phase advance errors between the interaction regions affected the DCI tune shift limit with two beams [9]. A simulation of DCI with two interaction regions and phase advance errors was performed to see if these errors affect the four-beam performance. These results are shown in Fig. 10. Phase advance errors between interaction points do not change the width of the stable region in this case.

The resonances bounding each of the regions as well as the resonances up to 30th order within each region are listed in Table III. In three of the regions (all except IV) one of the bounding resonances could be a lower, odd order resonance if the round beam symmetry were broken. In addition, two of the regions, I and IV, overlap resonances that could be lower odd order resonances, if the round beam symmetry were broken. Closed orbit offsets at the collision point or unequal horizontal and vertical tunes could break this symmetry and could possibly be the cause of the disagreement between measurements and this simulation.

## SUMMARY AND CONCLUSIONS

The simulation results are in excellent agreement with the qualitative features of Derbenev's theory: (i) absence of odd order resonances for round beams, (ii) tune dependence of the stability of the $f^+$ and $f^-$ modes, and (iii) phase space structure of the unstable modes. The widths and growth rates are comparable to those calculated, and the dependence on resonance order is in good agreement with that expected.

The simulation agrees with the locations of stable operating points in DCI, but predicts operating regions three to five times wider than those measured. There are a number of possible explanations, but they are difficult to explore because DCI is no longer available for colliding beam experiments.

High order coherent beam-beam instabilities have been observed with modest beam-beam strength parameter, $\xi \sim 0.02$–$0.04$; the width of an 18th order resonance was measured for Fig. 9, and the effects of 14th and 22nd order resonances are shown in Fig. 10. The appearance of these high order resonances is in contrast to the two-beam situation, where resonances higher than eighth order were never observed in simulation. The absence of Landau damping makes the coherent beam-beam interaction the important, limiting phenomena for space-charge-compensated colliding beams.

## ACKNOWLEDGMENTS

We wish to thank Alex Chao for his interest and comments and Sam Heifets for his help with solutions of the Vlasov equation. This work was supported by the Department of Energy, Contract No. DE-AC03-76SF00515.

[1] R. H. Siemann, *Frontiers of Particle Beams: Factories with $e^+e^-$ Rings,* edited by M. Dienes, M. Month, B. Strasser, and S. Turner, Lecture Notes in Physics Vol. 425 (Springer-Verlag, Berlin, 1994), p. 327.

[2] Ya. S. Derbenev, Nuclear Physics Institute, Siberian Division, Academy of Sciences of the USSR, Novosibirsk Report No. IYAF 70-72, 1972 (unpublished); Stanford Linear Accelerator Report No. SLAC TRANS 151, 1973 (unpublished).

[3] N. S. Dikansky and D. V. Pestrikov, Part. Accel. **12**, 27 (1982).

[4] A. Chao and R. Ruth, Part. Accel. **16**, 201 (1985).

[5] P. Zenkevich and K. Yokoya, Part. Accel. **40**, 229 (1993).

[6] S. Krishnagopal and R. Siemann, Phys. Rev. Lett. **67**,

2461 (1991).
[7] C. Bovet (private communication)
[8] J. Le Duff *et al.*, in *Proceedings of the 11th International Conference on High-Energy Accelerators,* edited by W. S. Newman (Birkhäuser Verlag, Basel, 1980), p. 707.
[9] S. Krishnagopal and R. Siemann, Nucl. Instrum. Methods Phys. Res. Sect. A **313**, 328 (1992).
[10] C. K. Birdsall and A. B. Langdon, *Plasma Physics via Computer Simulation* (McGraw-Hill, New York, 1985).
[11] IMSL MATH/LIBRARY, IMSL, Houston, TX, 1991.
[12] P. Craven and G. Wahba, Numer. Math. **31**, 377 (1979).
[13] J. Le Duff, M. P. Level, P. Marin, E. M. Sommer, and H. Zyngier (private communication).
[14] J. Le Duff and M. P. Level, Laboratoire de L'Accélérateur Linéaire Institution Report No. LAL/RT/80-03, 1980.